Noname manuscript No.
(will be inserted by the editor)

A realized volatility approach to option pricing with continuous and jump variance components

Dario Alitab · Giacomo Bormetti ·
Fulvio Corsi · Adam A. Majewski

Received: date / Accepted: date

Abstract Stochastic and time-varying volatility models typically fail to correctly price out-of-the-money put options at short maturity. We extend Realized Volatility option pricing models by adding a jump component which provides a rapidly moving volatility factor, and improves on the fitting properties under the physical measure. The change of measure is performed adopting a stochastic discount factor with an equity and two variance risk premia, associated to the continuous and jump components. Our choice preserves analytical tractability and offers a new way of separately estimate variance risk premia by coherently combining high-frequency returns and option data in a multi-factor pricing model.

Keywords High-frequency · Realized volatility · HARG · Option pricing · Variance risk premium · Jumps

1 Introduction

Stochastic and time-varying volatility models, such as [24, 35, 36], are able to qualitatively reproduce the smile (i.e. excess kurtosis) and the smirk (i.e. neg-

D. Alitab
Mediobanca S.p.A, Piazzetta E. Cuccia 1, 20121 Milano, Italy
E-mail: dario.alitab@gmail.com

G. Bormetti
University of Bologna, Piazza di Porta San Donato 5, 40126 Bologna, Italy
E-mail: giacomo.bormetti@unibo.it

F. Corsi
University of Pisa, via Ridolfi 10, 56100 Pisa, Italy
City University London, Northampton Square, London EC1V 0HB, United Kingdom
E-mail: fulvio.corsi@unipi.it

A. A. Majewski
Capital Fund Management, 23 Rue de l'Université, 75007 Paris, France
E-mail: aamajewski@gmail.com

ative skewness) observed in short term equity options. However, they fail to address these features quantitatively. As a result, they severely underprice out-of-the-money put options. To cope with this problem, a variety of models have been developed to include jumps in returns (see [7–9, 11, 13, 38, 39, 42, 43] in continuous-time, and [18, 25, 40] in discrete-time) and jumps in volatility (see, e.g., [10, 28, 29]). [17] employ a modified version of the two-factor component GARCH in [27] for option pricing, while [8] proposes a two-factor jump-diffusion model to fit the implicit distribution of options on Standard and Poor's 500 (S&P500) futures. Similarly, the family of Realized Volatility (RV) option pricing models recently proposed by [20] (i.e., ARG, HARG and HARGL) has difficulties in generating realistic level and dynamics of the steepness of the implied volatility at short maturity, although, the general shape and dynamics of the smile is much closer to the empirical one compared to the standard GARCH option pricing models. Therefore, the HARGL implies some degree of underpricing for deep out-of-the-money (DOTM) put options. This is a common feature of stochastic volatility option pricing models without jumps, since they cannot completely capture the probability mass in the right tail of the volatility density.

In this paper we extend the class of RV option pricing models by adding a jump component in volatility and its associated risk premium. The inclusion of jumps in the variance dynamics provides a rapidly moving volatility factor, which will improve on the fitting properties under the physical measure, $\mathbb{P}$, and on the pricing performance under the risk-neutral measure, $\mathbb{Q}$. Consequently, our change of measure employs an SDF with three different risk premia: one for equity, and two variance risk premia related to the continuous and jump components. The proposed multiple risk premia SDF allows to improve the flexibility of the option pricing model under the risk neutral dynamics while preserving analytical tractability. In addition, it provides a new methodology of separate estimation of the continuous and jump variance risk premia which coherently combines information from both high-frequency returns and option data. More specifically, we develop a model where the log-returns are determined by RV dynamics following a process belonging to the HAR-RV family. These processes, introduced by [19], successfully describe the impact that past realized variances aggregated on different time scales (daily, weekly and monthly) have on the current level of realized variance. Recently, [20] have studied the application of these discrete-time models to option pricing introducing the HARGL-RV extension which accounts for transition density specified by noncentered gamma distribution and accounts for the leverage effect through a daily binary component. More recently, [41] have widened the HARG-RV class and included a heterogeneous parabolic structure for leverage, defining the LHARG-RV model.

In this work, we extend the LHARG-RV model to account for a possibility of extreme movements in the evolution of volatility. The newly proposed model is labelled as JLHARG-RV. JLHARG-RV assumes that the dynamics of realized variance is given by the sum of two independent random variables which account for the continuous and the discontinuous components of the volatility. We model the former as an autoregressive gamma process (see [33]) whose conditional mean is assumed to be a linear function of the past realized variances and leverage terms aggregated over different time scales (daily, weekly, and monthly). The latter is described as a compound Poisson process where the jump size is sampled from a gamma distribution. For this model we first show how to compute analytically the moment generating function (MGF) of the log-returns, under the physical measure. In order to obtain an analytical option pricing formula, we derive the MGF under the risk neutral measure. The change of measure is performed adopting the same approach as in [17, 20, 31], based on a discrete-time exponential affine SDF which allows to incorporate risk premia for the continuous and discontinuous components of the volatility, in addition to the equity risk premium. We stress the importance of having risk premia for both the volatility factors in order to compensate for two new sources of risk, in addition to the traditional premium related to shocks in the log-return. In particular, including a premium for the jump component represents an important novel contribution of this work which helps to better understand the negative skew effect implied by out-of-the-money (OTM) option prices quoted on the market. Due to the analytical tractability of exponential-affine forms, we are able to derive the risk-neutral MGF and show that the risk-neutral model still belongs to the JLHARG model class. In particular, we prove the existence of a one-to-one mapping among the parameters describing the physical and risk-neutral dynamics of the JLHARG model. An additional advantage of JLHARG is related to the model estimation. This is due to the observability of RV, directly built from the high-frequency time series of log-returns. We compute the RV time series from tick-by-tick returns for the S&P500 futures, from January 1, 1990 to December 31, 2007. In order to separate the two dynamics of volatility, we exploit the Threshold Bipower Variation methodology introduced in [21] which allows to detect the jumps in the RV. Having the time-series for the continuous and discontinuous volatility components, we estimate the parameters of the JLHARG processes employing the Maximum Likelihood Estimator (MLE) on both sets of historical data.

To the best of our knowledge, among the approaches available in literature, [14] is the closest to ours. However, a closer look reveals several important differences. The first relevant difference is the method employed to identify and separate the continuous and jump components of the integrated variance. [14] compute a proxy of the continuous component of volatility by means of the Bipower Variation from 5-minute returns and the jump contribution corresponds to the difference, when positive, between the Realized Variance and the Bipower Variation. The methodology does not consider any statistical test in order to assess the significance of the jump contribution. The literature warns about the bias in the estimation of the continuous component of the integrated variance in finite sample, especially in presence of successive jump events. A second major difference is that the approach by Christoffersen and co-authors may be viewed as an improved and extended version of the Realized GARCH approach of [34], while the LHARG-ARJ extends the class of RV gamma models [20, 41]. The role played by the observable realized measures in the two classes is essentially different. In the former, the conditional variance is a latent process with idiosyncratic shocks given by the RV measure – in the same spirit of the Realized GARCH. The latter directly models the dynamics of the RV components. The impact of the two modeling choices is relevant not only on the estimation methodology – which is based on QMLE for the BPJVM and on MLE for the LHARG-ARJ – but also, and more importantly, on the level of persistence of the conditional variance in the two models. The persistence of the BPJVM latent variance is nearly one, then a miss-specification of the current level of the volatility may lead to the miss-fitting of the term structure of ATM implied volatility.

To assess the pricing performance of our model, we benchmark it with [14]. Our analysis is performed on OTM Plain Vanilla options written on S&P500 Index whose valuation is given each Wednesday from January 1, 1996 to December 31, 2004. We calibrate risk premia on the whole implied volatility surfaces and we compute the option prices using the efficient COS method introduced by [30]. Our results clearly illustrate that JLHARG models represent a valid competitor class to state-of-the-art discrete-time models for the valuation of S&P500 Index OTM options.

The rest of the paper is organized as follows. Section 2 defines our model for log-return and RV under both the physical and risk-neutral probability measures. Section 3 describes the estimation of the model and then analyses its statistical features. In Section 4, we discuss option pricing performances comparing them to the benchmark. Section 5 draws relevant conclusions.

2 The model

2.1 Real-World dynamics

We consider a risky asset with the following log-return dynamics

$$y_t = r + \left(\lambda - \frac{1}{2}\right) \mathrm{RV}_t + \sqrt{\mathrm{RV}_t}\epsilon_t, \tag{1}$$

where r is the risk-free rate, λ is the market price of risk[1], ϵ_t are *i.i.d.* standard normal innovations, and RV_t is realized variance at day t. The aggregate daily dynamics (1) is formally equivalent to that employed in [15, 20, 41]. As a major difference, in this paper we distinguish two separate components of realized variance: a continuous component RV_t^c and a jump component RV_t^j (details on the measurement of RV components are provided in Section 3).

Our approach is motivated by the empirical analyses of [1], who find that the distributions of daily equity returns standardized by the corresponding

[1] As shown in Appendix B, the more general specification

$$y_t = r + \lambda_c \mathrm{RV}_t^c + \lambda_j \mathrm{RV}_t^j + \sqrt{\mathrm{RV}_t^c + \mathrm{RV}_t^j}\epsilon_t \tag{2}$$

admits consistency with the no-arbitrage principle if and only if $\lambda_c = \lambda_j = \lambda$.

RV is approximately Gaussian and [2] who investigate the deviation from normality ascribed to a jump component in the price process. The latter results indicate that the discontinuous component has a minor impact on the distributional properties, since the jump-adjusted standardized series are not systematically closer to the Gaussian than the $y_t/\sqrt{RV_t}$ standardized returns.[2] This is especially true for time series generated from futures contracts on the S&P500 Index, which are recognized in [2] to suffer from minimal microstructure distortion and low liquidity effects. As can be seen from the density plots

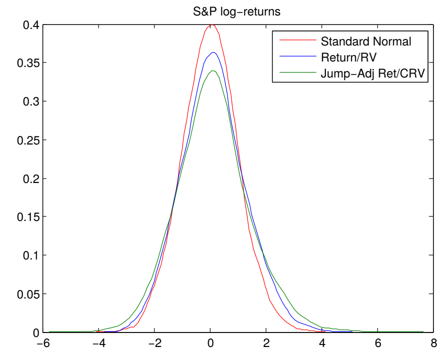

Fig. 1 Standardized log-return distribution. Comparison of the S&P500 futures log-return distribution under different scaling measures: Standard normal distribution (red line), jump-adjusted standardized log-return by RV^c (green line) and standardized log-return by total RV (blue line).

of Figure 1, we observe the same feature for the S&P500 futures in our sampling period. The two-sample Kolmogorov-Smirnov test between the RV standardized and jump-adjusted series indicates that the two distributions cannot be distinguished. If any, by judging on the value of the kurtosis of 3.64 for the jump-adjusted distribution and 3.06 for the RV standardized, we conclude that the latter is closer to a normal distribution than the former one.

Given the information at time t, $\mathcal{F}_t$, a new realization of the RV components is obtained by sampling at time $t+1$ from two conditionally independent distributions. The continuous part of RV depends on past realizations of RV^c and of a leverage component ℓ_t, which corresponds to a quadratic function of the total realized variance

$$\ell_t = \left(\epsilon_t - \gamma\sqrt{\mathrm{RV}_t^c + \mathrm{RV}_t^j}\right)^2 .$$

[2] *"Perhaps surprisingly, the results indicate that neither of the jump-adjusted standardized series are systematically closer to Gaussian than the non-adjusted realized volatility standardized returns. [...] One reason is that jumps largely self-standardize: a large jump tends to inflate the (absolute) value of both the return (numerator) and the realized volatility (denominator) of standardized returns, so the impact is muted"* [2].

Then, introducing the notation $\mathbf{RV^c}_t = (\mathrm{RV}^c_{t-21}, \ldots, \mathrm{RV}^c_t)$ and $\mathbf{L}_t = (\ell_{t-21}, \ldots, \ell_t)$, the continuous component of RV is drawn from a noncentred gamma distribution

$$\mathrm{RV}^c_{t+1}|\mathcal{F}_t \sim \bar{\gamma}(\delta, \Theta(\mathbf{RV^c}_t, \mathbf{L}_t), \theta)\,, \tag{3}$$

where δ is the shape parameter, and θ is the scale. The non-centrality is given by

$$\Theta(\mathbf{RV^c}_t, \mathbf{L}_t) = d + \beta_d \mathrm{RV}^{c\,(d)}_t + \beta_w \mathrm{RV}^{c\,(w)}_t + \beta_m \mathrm{RV}^{c\,(m)}_t + \alpha_d \ell^{(d)}_t + \alpha_w \ell^{(w)}_t + \alpha_m \ell^{(m)}_t\,, \tag{4}$$

where $d \in \mathbb{R}$, $\beta_i \in \mathbb{R}^+$, $\alpha_i \in \mathbb{R}^+$ are constant, and the quantities

$$\begin{array}{ll} \mathrm{RV}^{c\,(d)}_t = \mathrm{RV}^c_t, & \ell^{(d)}_t = \ell_t\,, \\ \mathrm{RV}^{c\,(w)}_t = \frac{1}{4}\sum_{i=1}^{4} \mathrm{RV}^c_{t-i}, & \ell^{(w)}_t = \frac{1}{4}\sum_{i=1}^{4} \ell_{t-i}\,, \\ \mathrm{RV}^{c\,(m)}_t = \frac{1}{17}\sum_{i=5}^{21} \mathrm{RV}^c_{t-i}, & \ell^{(m)}_t = \frac{1}{17}\sum_{i=5}^{21} \ell_{t-i} \end{array}$$

represent the heterogeneous components corresponding to the short-term or daily (d), medium-term or weekly (w) and long-term or monthly (m) realized variance and leverage terms, respectively on the left and right columns above.

The jump component of the realized variance is modelled as a compound Poisson process with intensity $\tilde{\Theta}$ and sizes sampled from a gamma distribution with shape $\tilde{\delta}$ and scale $\tilde{\theta}$

$$\mathrm{RV}^j_{t+1}|\mathcal{F}_t \sim \sum_{i=1}^{n_{t+1}} Y_i \quad \text{with} \quad n_{t+1} \sim \mathcal{P}(\tilde{\Theta}) \quad \text{and} \quad Y_i \; i.i.d. \sim \gamma(\tilde{\delta}, \tilde{\theta}). \tag{5}$$

Equations (1)-(5) completely characterise the log-return dynamics as an Autoregressive Gamma model in Realized Volatility with Heterogeneous Leverage and Jumps, and we acronym it JLHARG-RV model. The crucial advantage of the JLHARG model is that it satisfies the affine property. The importance of affine processes in finance - due to their analytical tractability - has been acknowledged in many studies (see [23, 26, 41] among others). We prove the following

Proposition 1 *Under $\mathbb{P}$, the MGF of the log-return $y_{t,T} = \sum_{k=t+1}^{T} y_k$ for JLHARG model has the following form*

$$\phi^{\mathbb{P}}(t, T, z) = \mathbb{E}^{\mathbb{P}}\left[e^{z y_{t,T}}|\mathcal{F}_t\right] = \exp\left(\mathrm{a}_t + \sum_{i=1}^{p} \mathrm{b}_{t,i} \mathrm{RV}^c_{t+1-i} + \sum_{i=1}^{q} \mathrm{c}_{t,i} \ell_{t+1-i}\right)\,,$$

where a_t, $\mathrm{b}_{t,i}$ and $\mathrm{c}_{t,i}$ are given by recursive relations.

Proof: See Appendix A.

2.2 Risk-neutralization

To preserve analytical tractability of the model under the martingale measure we employ an SDF within the family of exponential affine factors, whose high flexibility allows to incorporate multiple factor-dependent risk premia. This approach has been extensively used in literature.[3] We propose an SDF of the following form

$$M_{s,s+1} = \frac{e^{-\nu_c \mathrm{RV}^c_{s+1} - \nu_j \mathrm{RV}^j_{s+1} - \nu_y y_{s+1}}}{\mathbb{E}^{\mathbb{P}}\left[e^{-\nu_c \mathrm{RV}^c_{s+1} - \nu_j \mathrm{RV}^j_{s+1} - \nu_y y_{s+1}} | \mathcal{F}_s\right]}, \tag{6}$$

which represents the Esscher transform from the physical log-return density to the risk neutral one (see [12, 32]). The main advantage of the SDF (6) is to clearly identify the sources of risk and explicitly compensate them with separated risk premia. Specifically, this form allows to have both the continuous (ν_c) and discontinuous (ν_j) variance risk premia, in addition to the standard equity premium (ν_y). The equity premium has to satisfy the following no-arbitrage condition

Proposition 2 *The JLHARG model defined by equations (1) – (5) with SDF given by (6) satisfies the no-arbitrage condition if and only if*

$$\nu_y = \lambda + \frac{1}{2}.$$

Proof: Appendix B.

Moreover, we are able to provide a one-to-one mapping of the parameters under probability measure $\mathbb{P}$ to those under the $\mathbb{Q}$ measure, ensuring that the risk-neutral log-return dynamics is still governed by a JLHARG process.

Proposition 3 *Under risk-neutral measure $\mathbb{Q}$ the realized variance follows a JLHARG process with parameters*

$$\begin{aligned}
&\beta^*_d = \frac{\beta_d}{1-\theta \mathrm{y}^{c\,*}}, \quad \beta^*_w = \frac{\beta_w}{1-\theta \mathrm{y}^{c\,*}}, \quad \beta^*_m = \frac{\beta_m}{1-\theta \mathrm{y}^{c\,*}},\\
&\alpha^*_d = \frac{\alpha_d}{1-\theta \mathrm{y}^{c\,*}}, \quad \alpha^*_w = \frac{\alpha_w}{1-\theta \mathrm{y}^{c\,*}}, \quad \alpha^*_m = \frac{\alpha_m}{1-\theta \mathrm{y}^{c\,*}},\\
&\theta^* = \frac{\theta}{1-\theta \mathrm{y}^{c\,*}}, \quad \delta^* = \delta, \quad \gamma^* = \gamma + \lambda + \frac{1}{2}, \quad d^* = \frac{d}{1-\theta \mathrm{y}^{c\,*}},\\
&\tilde{\Theta}^* = \frac{\tilde{\Theta}}{\left(1-\tilde{\theta}\mathrm{y}^{j\,*}\right)^{\tilde{\delta}}}, \quad \tilde{\delta}^* = \tilde{\delta}, \quad \tilde{\theta}^* = \frac{\tilde{\theta}}{1-\tilde{\theta}\mathrm{y}^{j\,*}},
\end{aligned} \tag{7}$$

where $\mathrm{y}^{c\,*} = -\lambda^2/2 - \nu_c + \frac{1}{8}$ *and* $\mathrm{y}^{j\,*} = -\lambda^2/2 - \nu_j + \frac{1}{8}$.

[3] For example, in [3, 16, 20, 31, 41].

Proof: Appendix C.

Knowing the dynamics of the process under $\mathbb{Q}$, the moment generating function under the risk-neutral measure is a straightforward consequence of Proposition 1.

Corollary 1 *Under $\mathbb{Q}$ the MGF of the JLHARG model is formally the same as in Proposition 1 with equity risk premium $\lambda^* = -0.5$, and d^*, δ^*, θ^*, $\tilde{\Theta}^*$, $\tilde{\delta}^*$, $\tilde{\theta}^*$ γ^*, α_l^*, β_l^* for $l = d, w, m$ as in (7).*

We point out that the risk premia in the vector (ν_c, ν_j) are the only parameters that need to be calibrated on option data. Then, all the parameters governing the dynamics of the process under $\mathbb{Q}$ can be explicitly computed from the values estimated under $\mathbb{P}$ through the relations given by (7).

The JLHARG-RV family nests a variety of RV models as special cases. The first instance is the JHARG model which preserves the heterogeneous autoregressive structure for RV but lacks the leverage term. This model can be seen as a natural extension of the HARG model, by [20], accounting for a discontinuous component. The second model is the JLHARG model with Parabolic Leverage (P-JLHARG) that we obtain setting $d = 0$ in (4). The third one is a JLHARG with zero-mean leverage term (ZM-JLHARG) inspired by the Component GARCH model of [17]. In that case, heterogeneous leverage components are given by the following relations

$$\begin{aligned}
\bar{\ell}_t^{(d)} &= \epsilon_t^2 - 1 - 2\epsilon_t \gamma \sqrt{\mathrm{RV}_t^c + \mathrm{RV}_t^j}, \\
\bar{\ell}_t^{(w)} &= \frac{1}{4} \sum_{i=1}^{4} \left(\epsilon_{t-i}^2 - 1 - 2\epsilon_{t-i} \gamma \sqrt{\mathrm{RV}_{t-i}^c + \mathrm{RV}_{t-i}^j} \right), \\
\bar{\ell}_t^{(m)} &= \frac{1}{17} \sum_{i=5}^{21} \left(\epsilon_{t-i}^2 - 1 - 2\epsilon_{t-i} \gamma \sqrt{\mathrm{RV}_{t-i}^c + \mathrm{RV}_{t-i}^j} \right).
\end{aligned}$$

The linear $\Theta(\mathbf{RV^c}_t, \mathbf{L}_t)$ reads

$$\beta_d \mathrm{RV}_t^{c(d)} + \beta_w \mathrm{RV}_t^{c(w)} + \beta_m \mathrm{RV}_t^{c(m)} + \alpha_d \bar{\ell}_t^{(d)} + \alpha_w \bar{\ell}_t^{(w)} + \alpha_m \bar{\ell}_t^{(m)},$$

which can be reduced to the form (4) setting $d = -(\alpha_d + \alpha_w + \alpha_m)$, $\beta_l = \beta_l - \alpha_l \gamma^2$ for $l = d, w, m$. The larger flexibility of the leverage term $\bar{\ell}_t$ allows the model to better describe the skewness and kurtosis of the empirical data.

3 Model estimation and statistical properties

The estimation of the parameter under $\mathbb{P}$ is greatly simplified by the direct observability of RV which avoids the need of latent volatility filtering. In this paper, the RV time series is obtained from tick-by-tick data for the S&P500 futures, from January 1, 1990 to December 31, 2007. Our estimation procedure for the continuous and jump component is the following:

i) we estimate the total quadratic variation of the log-prices using the Two-Scale estimator introduced by [45];
ii) we identify the discontinuous component using the Threshold Bipower variation method by [21] which detects the spikes in RV time series and separates it from the continuous component.

The RV, so far defined, is built from open-to-close data, thus neglecting the overnight contribution. We adjust our RV estimator by rescaling the time series so to match the unconditional mean of the squared daily returns (close-to-close). We stress that the adopted jump detection method, according to point (ii) of our procedure, represents a formal statistical test based on asymptotic theory. This is important to statistically identify days with jumps and subsequently associate the most extreme intra-day price movements to jump events (see for instance [2, 4, 5, 21, 37]).

Having the time series for the RV components and log-returns, we can estimate the parameters of the JLHARG-RV processes via MLE. According to the model specified in equation (3) and (5), the log-likelihood functions for the continuous and jump RV components, respectively $l^c_{t,T}$ and $l^j_{t,T}$, are given by the following series-expansions

$$l^c_{t,T}\left(\lambda,\delta,\theta,d,\beta_d,\beta_w,\beta_m,\alpha_d,\alpha_w,\alpha_m,\gamma\right) = -\sum_{t=1}^{T}\left(\frac{\mathrm{RV}^c_t}{\theta} + \Theta\left(\mathbf{RV^c}_{t-1},\mathbf{L}_{t-1}(\lambda)\right)\right)$$
$$+\sum_{t=1}^{T}\log\left(\sum_{k=1}^{\infty}\frac{(\mathrm{RV}^c_t)^{\delta+k-1}}{\theta^{\delta+k}\Gamma\left(\delta+k\right)}\frac{\Theta\left(\mathbf{RV^c}_{t-1},\mathbf{L}_{t-1}(\lambda)\right)^k}{k!}\right),$$

$$l^j_{t,T}\left(\tilde{\delta},\tilde{\theta},\tilde{\Theta}\right) = -\sum_{t=1}^{T}\left(\frac{\mathrm{RV}^j_t}{\tilde{\theta}} + \tilde{\Theta}\right) + \sum_{t=1}^{T}\log\left(\sum_{k=1}^{\infty}\frac{\left(\mathrm{RV}^j_t\right)^{k\tilde{\delta}-1}}{\theta^{k\tilde{\delta}}\Gamma\left(k\tilde{\delta}\right)}\frac{\tilde{\Theta}^k}{k!}\right).$$

Both log-likelihoods have a term involving an infinite series. To overcome this issue we operate a truncation of the infinite sum to the $90th$ order as suggested in [20]. The log-likelihood function of returns reads

$$l^r_{t,T}(\lambda) = -\sum_{t=1}^{T}\left(\frac{\left(y_t - r - \left(\frac{1}{2}-\lambda\right)\left(\mathrm{RV}^c_t + \mathrm{RV}^j_t\right)\right)^2}{2(\mathrm{RV}^c_t + \mathrm{RV}^j_t)} + \frac{1}{2}\log(2\pi(\mathrm{RV}^c_t + \mathrm{RV}^j_t))\right).$$

The estimation of the parameters is performed maximizing the whole log-likelihood function $l_{t,T}(\boldsymbol{\theta}) = l^c_{t_T} + l^j_{t_T} + l^r_{t_T}$, with $\boldsymbol{\theta} = (\lambda,\delta,\theta,d,\beta_d,\beta_w,\beta_m,\alpha_d,\alpha_w,\alpha_m,\gamma,\tilde{\delta},\tilde{\theta},\tilde{\Theta})$. In order to reduce the dimension of the space of parameters, we fix δ and $\tilde{\delta}$ by variance targeting, i.e. matching the sample mean of the realized variance. Fed Funds rate are employed as proxy for the risk-free rate r.

Parameter	JHARG	P-JLHARG	ZM-JLHARG	Parameter	BPJVM
λ	2.74 (1.50)	2.38 (1.59)	2.69 (1.55)	λ_z	1 (4)
θ	9.75e-06 (9e-08)	9.1e-06 (1e-07)	9.5e-06 (1e-07)	λ_y	4e-05 (8e-05)
δ	1.36	1.25	1.83	γ	1.44e+04 (2e+02)
β_d	4.67e+04 (8e+02)	3.5e+04 (2e+03)	3.9e+04 (1e+03)	ω_z	2.5e-08
β_w	2.9e+04 (1e+03)	3.2e+04 (2e+03)	2.9e+04 (2e+03)	ω_y	0.04
β_m	1.19e+04 (9e+02)	1.4e+04 (3e+03)	1.8e+04 (2e+03)	σ	1.86e-07 (2e-09)
α_d	-	0.28 (0.03)	0.44 (0.04)	θ	1e-05 (5e-05)
α_w	-	0.07 (0.03)	0.42 (0.06)	δ	1.28e-03 (1e-05)
α_m	-	0.00 (0.06)	0.52 (0.10)	ρ	3.3e-01 (2e-02)
γ	-	173 (16)	120 (12)	b_z	6.5e-01 (3e-02)
$\tilde{\theta}$		4.7e-05 (3e-06)		b_y	9.5e-01 (1e-02)
$\tilde{\delta}$		1.15		a_z	3.5e-01 (3e-02)
$\tilde{\Theta}$		0.299 (0.009)		a_y	2.2e+04 (5e+03)
ν_c	756	-1440	-2466		-807
ν_j	-12396	-10239	-7609		-64550
Log-likelihood	10575	10248	10220	Persistence$_z$	0.999
Persistence	0.85	0.82	0.81	Persistence$_y$	0.986

Table 1 Maximum likelihood estimates, standard errors, and log-likelihood values. The historical data for the JHARG, P-JLHARG, ZM-JLHARG, and BPJVM models are given by the daily RV computed on tick-by-tick data for the S&P500 futures. For all models, the estimation period ranges from 1990 to 2007.

In Table 1, first four columns, the parameter values estimated under $\mathbb{P}$ are reported. We present estimates for three different models JHARG, P-JLHARG and ZM-JLHARG together with the standard deviations and log-likelihood values. Our results confirm that the impact of the past RV^c components on the current level of RV decreases with the increase of the aggregation horizon. The same evidence has been documented by [19, 22, 41]. Skewness and kurtosis term structures of the underlying distribution play an important role in reproducing the shape of the implied volatility surface and option pricing. Adding a heterogeneous leverage considerably improves the skewness and the excess kurtosis of the log-return probability distribution. In this paper, we not only preserve the heterogeneity of the leverage, but we also add a discontinuous component which captures extreme price movements. With this choice, our JLHARG class of models is able to reproduce a stronger leverage effect. In Figure 2 we show the skewness and the excess kurtosis from a simulation of the P-JLHARG model with parameters from Table 1 at different aggregation time – from one 1 day to 250 days – under both $\mathbb{P}$ and $\mathbb{Q}$ measures. The model is able to reproduce significant negative values of skewness and positive excess kurtosis under the physical measure. When moving to the $\mathbb{Q}$ measure, the effect is strengthened by the presence of the variance risk premia ν_c and ν_j.

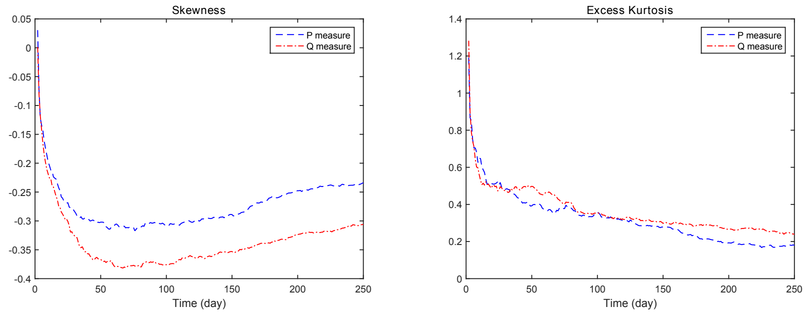

Fig. 2 Skewness and excess kurtosis of the JLHARG process under physical and risk-neutral measures.

4 Option valuation

Our data set consists of Plain Vanilla OTM options on S&P500 Index for each Wednesday from January 1, 1996 to December 31, 2004. We first apply a standard filter removing options with maturity less than 10 days or more than 365 days, implied volatility larger than 70% and prices less than 0.05$ (see [6], [20] and [41]). Using K/S_t as definition of moneyness, we filter out DOTM options with moneyness larger than 1.3 for call options and less than 0.7 for put options. This choice yields a total number of 46066 observations. For our purposes, put options are identified as DOTM if their moneyness is between $0.7 \leq m \leq 0.9$ and OTM if $0.9 < m \leq 0.98$. On the other hand, call options are said to be DOTM if $1.1 < m \leq 1.3$ and OTM if $1.02 < m \leq 1.1$. Options are called at-the-money (ATM) if $0.98 < m \leq 1.02$. As far as the time to maturity τ is concerned, we identify options as short maturity ($\tau \leq 50$ days), short-medium maturity ($50 < \tau \leq 90$ days), long-medium maturity ($90 < \tau \leq 160$ days), and long maturity ($\tau > 160$ days).

4.1 Model calibration and pricing method

In order to derive the risk-neutral dynamics, the values of risk premium parameters (ν_c, ν_j, ν_y) need to be identified. According to Proposition 2, ν_y is fixed by the no-arbitrage condition, while ν_c and ν_j remain as free parameters to be calibrated on option prices.

Calibration procedure is based on the unconditional minimization of the distance between the market implied and the model implied volatility surface. For this reason, we divide our dataset in different intervals of moneyness and maturity obtaining a 5×4 moneyness-maturity grid. Then, for each subset, we compute the unconditional mean of the market implied volatilities.

In this way, as shown in Table 2, we obtain a 20-point discrete representation of the implied volatility surface. Finally, we compute the same discrete grid

Moneyness	Maturity $\tau \leq 50$	$50 < \tau \leq 90$	$90 < \tau \leq 160$	$160 < \tau$
	Implied Volatility			
$0.7 \leq m \leq 0.9$	0.3564	0.3056	0.2866	0.2662
$0.9 < m \leq 0.98$	0.2353	0.2269	0.2232	0.2230
$0.98 < m \leq 1.02$	0.1958	0.2023	0.2059	0.2108
$1.02 < m \leq 1.1$	0.1767	0.1790	0.1849	0.1923
$1.1 < m \leq 1.3$	0.2317	0.1946	0.1836	0.1842

Table 2 Mean market implied volatilities of S&P500 Index options on each Wednesday from January 1,1996 to December 31, 2004 (46066 observations) sorted by moneyness and maturity. Moneyness is defined as $m = K/S_t$, where K and S_t are the strike and the underlying price, respectively. Maturity is measured in calendar days.

for the model implied volatility and we identify the optimal values of (ν_c, ν_j) which minimize the distance between the two grids, i.e.

$$\arg\min_{(\nu_c,\nu_j)} \{f_{\text{obj}}(\nu_c, \nu_j)\} .$$

The objective function $f_{\text{obj}}(\nu_c, \nu_j)$ is defined as

$$f_{\text{obj}}(\nu_c, \nu_j) = \sqrt{\sum_{i=1}^{5} \sum_{j=1}^{4} \left(\text{IV}_{ij}^{\text{mod}} (\nu_c, \nu_j) - \text{IV}_{ij}^{\text{mkt}} \right)^2},$$

and represents the quadratic distance between the model implied volatility surface and the market one, whose elements are $\text{IV}_{ij}^{\text{mod}} (\nu_c, \nu_j)$ and $\text{IV}_{ij}^{\text{mkt}}$, respectively. In order to compute the option prices – and associated implied volatilities – we employ a numerical scheme introduced by [30], termed the COS method. This method, based on Fourier-cosine expansions, efficiently evaluates the price of Plain Vanilla options from the characteristic function of log-returns.

At the bottom of Table 1 we report the calibrated variance risk premia for JHARG models. It is worth recalling that the presence of a positive or a negative value of the risk premium reduces or amplifies the unconditional mean of realized variance, respectively. Moreover, negative premia have the genuine effect to induce more skew in the distribution of returns. The risk premium, ν_c, associated with the continuous component varies from the positive value of the JHARG model to a large negative value for the ZM-JLHARG model. The risk premia, ν_j, associated with the jump component, are all negative and increasing (decreasing in absolute terms) when a better specified form of the leverage is adopted. The most negative jump premium corresponds to the JHARG model and decreases for the P-JLHARG with heterogeneous parabolic leverage. It reaches the highest value (smallest in absolute terms) for the ZM-JLHARG where the heterogeneous leverage is centred. The compensation taking place between ν_c and ν_j is due to the fact that large negative innovations in the price rise the future variance through the leverage term. Then, a better specification of the leverage component reduces the relative weight of the jump premium in favour of the premium of the continuous component.

4.2 Pricing results

We can summarize the option pricing procedure in four steps: (i) estimation of the parameters under the physical measure $\mathbb{P}$; (ii) unconditional calibration of the parameter vector (ν_c, ν_j); (iii) mapping of parameter values from $\mathbb{P}$ to $\mathbb{Q}$ using expressions (7); (iv) numerical computation of option prices through COS method using the MGF recursive formulas in (17).

As benchmark approach to assess the pricing performance of JHARG models, we use the BiPower Jump Variation Model (BPJVM) introduced by [14].[4] The BPJVM model is a state-of-the-art approach incorporating a GARCH structure for the latent volatility and jump intensity where bipower and jump variations play a prominent role as idiosyncratic components. To ensure a fair comparison with the ZM-JLHARG, risk-neutralization is achieved by means of a four-dimensional Esscher transform. Two risk premia compensate for the realized variance components - as in (6) - and two auxiliary premia, μ_c and μ_j, compensate for the continuous and jump return components. The former two parameters have to be calibrated on option data, while the latter are fixed by no-arbitrage. All computational details are available from authors upon request. The last two columns of Table 1 report the parameter values for the BPJVM. Following [14], estimation is performed via quasi-maximum likelihood. At variance with them, we solely use the physical information, and only afterwards we calibrate the free parameters ν_c and ν_j on market option prices. This choice is motivated by consistency with the approach proposed in this paper. Here, we first estimate the physical parameters from historical information and then we separately assess the impact of risk compensation on the risk neutral dynamics.

As customary in literature ([20, 41, 44]), we employ the Root Mean Square Error (RMSE) on the percentage IV as performance measure, i.e.

$$RMSE_{IV} = \sqrt{\sum_{i=1}^{N} \frac{\left(IV_i^{mod} - IV_i^{mkt}\right)^2}{N}},$$

where N is the number of options, and IV^{mod} and IV^{mkt} are the model and the market implied volatility, respectively.

Preceding comparison with benchmark models, we perform an internal horse-race to select the best candidate among JHARG models. In Table 3 we report the global comparison of the option pricing performances between models belonging to the JHARG class. We build ratios between the RMSE of each couple

[4] For practical implementation, we refer to the updated version available on SSRN including some corrections to the published version. Link: http://ssrn.com/abstract=2494379.

Implied Volatility RMSE

	Moneyness	
Model	$0.9 < m < 1.1$	$0.7 < m < 1.3$
JHARG	4.89	6.65
P-JLHARG/JHARG	0.91	0.93
ZM-JLHARG/JHARG	0.83	0.85
ZM-JLHARG/P-JLHARG	0.91	0.92
ZM-JLHARG/BPJVM	0.81	0.83

Table 3 Global option pricing performance for the JLHARG class of models and comparison with the BPJVM model on S&P500 options from January 1, 1996 to December 31, 2004. The RV measure is estimated from 1990 to 2007. Parameter estimates are taken from Table 1.

of models. The table shows that – in terms of RMSE – the performance improves for models accounting for the leverage effect, as expected. Specifically, fixing as benchmark the JHARG model with no leverage, performances in the range of moneyness $0.9 < m < 1.1$ improve by nearly 9% for P-JLHARG and by 17% for ZM-JLHARG. In the range of moneyness $0.7 < m < 1.3$ the improvements are by 7% and by 15% for P-JLHARG and ZM-JLHARG, respectively. These results confirm the well established fact that the inclusion of a leverage component is essential for option pricing. Moreover, ZM-JLHARG always outperforms P-JLHARG independently on the range of moneyness. In accordance with [41] this finding reaffirms that the zero-mean leverage shows more flexibility with respect to the parabolic leverage. The final row of Table 3 reveals the superior performance of the ZM-JLHARG model when benchmarked with the BPJVM. Gains in performance vary from 19%, in the range of moneyness close to ATM, to 17%, when more extreme moneyness are included. The result for the central region of the volatility surface confirms that the heterogeneous structure is a parsimonious and effective way to provide a satisfactory description of the ATM implied volatility dynamics.

In Table 4, the focus is on a more detailed comparison between the ZM-JLHARG model and the competitor BPJVM. Dividing the entire dataset of options according to the grid used for model calibration (see Section 4.1), we observe that for short maturities $\tau \leq 50$ the two models price with almost the same accuracy in the at-the-money region $0.98 < m < 1.02$. BPJVM increases the pricing performance for OTM call options but for DOTM calls the ZM-JLHARG performs better by a factor of 0.71. In the region of short-maturity puts the ZM-JLHARG model consistently over-performs the competitor BPJVM. This result is confirmed with slightly different percentages for options with medium-short maturity $50 < \tau \leq 90$ noting a worsening of BPJVM performance in the ATM region with respect to ZM-JLHARG. As concerns the medium-long maturity region $90 < \tau \leq 160$ BPJVM maintains a higher performance in pricing OTM calls and shows a better valuation of DOTM puts than the ZM-JLHARG. Finally, valuation of long maturity options exhibits the consistent over-performance of the ZM-JLHARG model for

	Maturity			
Moneyness	$\tau \leq 50$	$50 < \tau \leq 90$	$90 < \tau \leq 160$	$160 < \tau$
Panel A	ZM-JLHARG Implied Volatility RMSE			
$0.7 \leq m \leq 0.9$	12.02	7.53	6.06	4.93
$0.9 < m \leq 0.98$	4.02	3.55	3.72	4.09
$0.98 < m \leq 1.02$	3.43	3.71	4.01	4.52
$1.02 < m \leq 1.1$	4.13	4.59	4.79	4.96
$1.1 < m \leq 1.3$	4.70	3.93	4.58	5.10
Panel B	ZM-JLHARG/BPJVM Implied Volatility RMSE			
$0.7 \leq m \leq 0.9$	0.89	1.05	1.19	0.71
$0.9 < m \leq 0.98$	0.72	0.81	0.85	0.59
$0.98 < m \leq 1.02$	1.02	0.91	0.89	0.67
$1.02 < m \leq 1.1$	1.03	1.02	0.95	0.63
$1.1 < m \leq 1.3$	0.71	0.61	0.58	0.45

Table 4 Panel A: Percentage $RMSE_{IV}$ of the ZM-JLHARG model sorted by moneyness and maturity. Panel B: $RMSE_{IV}$ ratios computed using BPJVM as benchmark model.

both puts and calls covering all ranges of moneyness under study. The smaller error of ZM-JLHARG for long maturity options suggests that this model has more flexibility than BPJVM to reproduce a realistic term structure of implied volatilities. A possible reason for the rigidity of BPJVM could be the extremely high persistence of both volatility and jump intensity processes, as reported in Table 1. High persistence is a crucial feature to reproduce the long-memory property of the volatility process, nevertheless an extreme level could have the side effect of systematical miss-valuing options – either over-pricing or under-pricing depending on the prevailing high or low level of volatility, respectively.

5 Conclusions

In this paper, we present a class of heterogeneous autoregressive models accounting for a discontinuous component in Realized Volatility. We demonstrate how to analytically characterize the moment generating function of the log-return process under physical and risk-neutral measure. Risk-neutralization is done with a flexible exponential affine pricing kernel which identifies different risks and separately compensates for them introducing three components of risk premium: equity, continuous and jump variance. Then, we show the improvements of the novel class of models in reproducing different features of the implied volatility surface compared with the state-of-the-art of discrete-time pricing models encompassing both continuous and jump dynamics of underlying assets.

As a future perspective, we are aware that equation (5) implicitly assumes that the jump intensity is constant. A stream of literature – consider for instance the empirical conclusions drawn in [14] – advocates an extension considering a time-varying jump intensity. This development is left for future research. Nonetheless, the current contribution shows the ability of JLHARG model to over-perform the benchmark BPJVM model. Moreover, the degree of jump persistence under P measure strongly depends on the methodology employed for the jump identification. We believe that testing for the presence of jumps is an important step for a correct identification procedure. This could partially prevent for over-identification and contamination of the jump component with persistence due to the continuous component.

References

1. Andersen, T.G., Bollerslev, T., Diebold, F., Ebens, H.: The distribution of stock returns volatilities. Journal of Financial Economics **61**, 43–76 (2001)
2. Andersen, T.G., Bollerslev, T., Frederiksen, P., Ørregaard Nielsen, M.: Continuous-time models, realized volatilities, and testable distributional implications for daily stock returns. Journal of Applied Econometrics **25**(2), 233–261 (2010)
3. Bandi, F.M., Renò, R.: Price and volatility co-jumps. Journal of Financial Economics **119**, 107 – 146 (2016)
4. Barndorff-Nielsen, O.E., Shephard, N.: Power and bipower variation with stochastic volatility and jumps. Journal of Financial Econometrics **2**(1), 1–37 (2004)
5. Barndorff-Nielsen, O.E., Shephard, N.: Econometrics of testing for jumps in financial economics using bipower variation. Journal of Financial Econometrics **4**(1), 1–30 (2006)
6. Barone-Adesi, G., Engle, R., Mancini, L.: A GARCH option pricing with filtered historical simulation. Review of Financial Studies **21**, 1223–1258 (2008)
7. Bates, D.: Jumps and stochastic volatility: Exchange rate processes implicit in Deutsche mark options. Review of Financial Studies **9**, 69–107 (1996)
8. Bates, D.: Post-'87 crash fears in the S&P 500 futures option market. Journal of Econometrics **94**(1-2), 181–238 (2000)
9. Bates, D.: Maximum likelihood estimation of latent affine processes. Review of Financial Studies **19**, 909–965 (2006)
10. Broadie, M., Chernov, M., Johannes, M.: Model specification and risk premia: evidence from futures options. Journal of Finance **62**, 1453–1490 (2007)
11. Broadie, M., Detemple, J.B.: Anniversary article: Option pricing: Valuation models and applications. Management Science **50**(9), 1145–1177 (2004)
12. Bühlmann, H., Delbaen, F., Embrechts, P., Shiryaev, A.N.: No-arbitrage, change of measure and conditional esscher transforms. CWI quarterly **9**(4), 291–317 (1996)
13. Cai, N., Kou, S.G.: Option pricing under a mixed-exponential jump diffusion model. Management Science **57**(11), 2067–2081 (2011)
14. Christoffersen, P., Fenou, B., Jeon, Y.: Option valuation with observable volatility and jump dynamics. Journal of Banking & Finance **61**(Supplement 2), S101–S120 (2015)
15. Christoffersen, P., Feunou, B., Jacobs, K., Meddahi, N.: The economic value of realized volatility: Using high-frequency returns for option valuation. Journal of Financial and Quantitative Analysis **49**(03), 663–697 (2014)
16. Christoffersen, P., Heston, S., Jacobs, K.: Capturing option anomalies with a variance-dependent pricing kernel. Review of Financial Studies **26**(8), 1962–2006 (2013)
17. Christoffersen, P., Jacobs, K., Ornthanalai, C., Wang, Y.: Option valuation with long-run and short-run volatility components. Journal of Financial Economics **90**(3), 272–297 (2008)
18. Christoffersen, P., Redouane, E., Fenou, B., Jacobs, K.: Options valuation with conditional heteroskedasticity and non-normality. Review of Financial Studies **23**, 2139–2183 (2010)

19. Corsi, F.: A simple approximate long-memory model of realized-volatility. Journal of Financial Econometrics **7**, 174–196 (2009)
20. Corsi, F., Fusari, N., La Vecchia, D.: Realizing smiles: Options pricing with realized volatility. Journal of Financial Economics **107**(2), 284–304 (2013)
21. Corsi, F., Pirino, D., Renò, R.: Threshold bipower variation and the impact of jumps on volatility forecasting. Journal of Econometrics **159**(2), 276 – 288 (2010)
22. Corsi, F., Renò, R.: Discrete-time volatility forecasting with persistent leverage effect and the link with continuous-time volatility modeling. Journal of Business & Economic Statistics **30**(3), 368–380 (2012)
23. Darolles, S., Gourieroux, C., Jasiak, J.: Structural laplace transform and compound autoregressive models. Journal of Time Series Analysis **27**, 477–503 (2006)
24. Duan, J.C.: The GARCH option pricing model. Mathematical Finance **5**, 13–32 (1995)
25. Duan, J.C., Ritchken, P., Sun, Z.: Approximating garch-jump models, jump-diffusion processes, and option pricing. Mathematical Finance **16**, 21–52 (2006)
26. Duffie, D., Pan, J., Singleton, K.: Transform analysis and asset pricing for affine jump-diffusions. Econometrica **68**, 1343–1376 (2000)
27. Engle, R., Lee, G.: A permanent and transitory component model of stock return volatility, in ed. R. Engle and H. White Cointegration, Causality, and Forecasting: A Festschrift in Honor of Clive W. J. Granger (1999)
28. Eraker, B.: Do stock prices and volatility jump? Reconciling evidence from spot and option prices. Journal of Finance **59**, 1367–1403 (2004)
29. Eraker, B., Johannes, M., Polson, N.: The impact of jumps in volatility and returns. Journal of Finance **58**, 1269–1300 (2003)
30. Fang, F., Oosterlee, C.W.: A novel pricing method for european options based on Fourier-Cosine series expansions. SIAM Journal on Scientific Computing **31**, 826–848 (2008)
31. Gagliardini, P., Gouriéroux, C., Renault, E.: Efficient derivative pricing by the extended method of moments. Econometrica **79**(4), 1181–1232 (2011)
32. Gerber, H.U., Shiu, E.S.: Option pricing by esscher transforms. Transactions of the Society of Actuaries **46**(99), 140 (1994)
33. Gourieroux, C., Jasiak, J.: Autoregressive gamma process. Journal of Forecasting **25**, 129–152 (2006)
34. Hansen, P.R., Huang, Z., Shek, H.H.: Realized GARCH: a joint model for returns and realized measures of volatility. Journal of Applied Econometrics **27**(6), 877–906 (2012)
35. Heston, S.: Options with stochastic volatiltiy with applications to bond and currency options. The Review of Fiancial Studies **6**, 327–343 (1993)
36. Heston, S., Nandi, S.: A closed-form GARCH option valuation model. Review of Financial Studies **13**(3), 585–625 (2000)
37. Huang, X., Tauchen, G.: The relative contribution of jumps to total price variance. Journal of Financial Econometrics **3**(4), 456–499 (2005)
38. Huang, X., Wu, L.: Specification analysis of option pricing model s base on time-changed Lévy processes. Journal of Finance **59**, 1405–1439 (2004)
39. Kou, S.G.: A jump-diffusion model for option pricing. Management Science **48**(8), 1086–1101 (2002)
40. Maheu, J., McCurdy, T.: News arrival, jump dynamics and volatility components for individual stock returns. Journal of Finance **59**, 755–793 (2004)
41. Majewski, A.A., Bormetti, G., Corsi, F.: Smile from the past: A general option pricing framework with multiple volatility and leverage components. Journal of Econometrics **187**(2), 521–531 (2015)
42. Merton, R.C.: Option pricing when underlying stock returns are discontinuosus. Journal of Financial Economics **3**, 125–144 (1976)
43. Pan, J.: The jump-risk premia implicit in options: Evidence from an integrated time-series study. Journal of Financial Economics **63**, 3–50 (2002)
44. Renault, E.: Econometric models of option pricing errors. Econometric Society Monographs **28**, 223–278 (1997)
45. Zhang, L., Aït-Sahalia, Y., Mykland, P.A.: A tale of two time scales: Determining integrated volatility with noisy high frequency data. Journal of the American Statistical Association **100**, 1394–1411 (2005)

A MGF under $\mathbb{P}$ measure

The relations which follow are derived for the log-return dynamics specified in Eq. (2). For the ease of computation, the expression (4) is rewritten as

$$\Theta(\mathbf{RV^c}_t, \mathbf{L}_t) = d + \sum_{i=1}^{22} \beta_i \mathrm{RV}^c_{t+1-i} + \sum_{i=1}^{22} \alpha_i \left(\epsilon_{t+1-i} - \gamma \sqrt{\mathrm{RV}^c_{t+1-i} + \mathrm{RV}^j_{t+1-i}} \right)^2 ,$$

with

$$\beta_i = \begin{cases} \beta_d & \text{for } i = 1 \\ \beta_w/4 & \text{for } 2 \leq i \leq 5 \\ \beta_w/17 & \text{for } 6 \leq i \leq 22 \end{cases} \qquad \alpha_i = \begin{cases} \alpha_d & \text{for } i = 1 \\ \alpha_w/4 & \text{for } 2 \leq i \leq 5 \\ \alpha_w/17 & \text{for } 6 \leq i \leq 22 \end{cases} . \tag{8}$$

We start showing that JLHARG processes satisfy the affine relation

$$\mathbb{E}\left[e^{zy_{s+1} + \mathbf{b}\cdot\mathbf{RV}_{s+1} + c\ell_{s+1}} | \mathcal{F}_s\right] = e^{\mathcal{A}(z,\mathbf{b},c) + \sum_{i=1}^{p} \boldsymbol{\mathcal{B}}_i(z,\mathbf{b},c)\cdot\mathbf{RV}_{s+1-i} + \sum_{j=1}^{q} \mathcal{C}_j(z,\mathbf{b},c)\ell_{s+1-j}} , \tag{9}$$

for some functions $\mathcal{A} : \mathbb{R}\times\mathbb{R}^2\times\mathbb{R} \to \mathbb{R}$, $\boldsymbol{\mathcal{B}}_i : \mathbb{R}\times\mathbb{R}^2\times\mathbb{R} \to \mathbb{R}^2$, $\boldsymbol{\mathcal{C}}_j : \mathbb{R}\times\mathbb{R}^2\times\mathbb{R} \to \mathbb{R}$, where $\mathbf{RV}_t = (\mathrm{RV}^c_t, \mathrm{RV}^j_t)$, $\mathbf{b} \in \mathbb{R}^2$, $c \in \mathbb{R}$, and $\cdot$ is the scalar product in $\mathbb{R}^2$. To derive the explicit form of the functions $\mathcal{A}$, $\mathcal{B}_i$, $\mathcal{C}_j$ which allows to characterise the MGF we show that

$$\begin{aligned}
&\mathbb{E}^{\mathbb{P}}\left[\mathrm{e}^{zy_t + \mathbf{b}\cdot\mathbf{RV}_t + c\ell_t} | \mathcal{F}_{t-1}\right] \\
&= \mathbb{E}^{\mathbb{P}}\left[\mathrm{e}^{z(r + \lambda_c \mathrm{RV}^c_t + \lambda_j \mathrm{RV}^j_t + \sqrt{\mathrm{RV}^c_t + \mathrm{RV}^j_t}\epsilon_t) + \mathbf{b}\cdot\mathbf{RV}_t + c\ell_t} | \mathcal{F}_{t-1}\right] \\
&= \mathbb{E}^{\mathbb{P}}\left[\mathrm{e}^{z(r + \lambda_c \mathrm{RV}^c_t + \lambda_j \mathrm{RV}^j_t) + \mathbf{b}\cdot\mathbf{RV}_t} \mathbb{E}^{\mathbb{P}}\left[\mathrm{e}^{z\sqrt{\mathrm{RV}^c_t + \mathrm{RV}^j_t}\epsilon_t + c(\epsilon_t - \gamma\sqrt{\mathrm{RV}^c_t + \mathrm{RV}^j_t})^2} | \mathbf{RV}_t\right] | \mathcal{F}_{t-1}\right] \\
&= \mathbb{E}^{\mathbb{P}}\left[\mathrm{e}^{z(r + \lambda_c \mathrm{RV}^c_t + \lambda_j \mathrm{RV}^j_t) + b_1 \mathrm{RV}^c_t + b_2 \mathrm{RV}^j_t - \frac{1}{2}\ln(1-2c) + \left(\frac{\frac{z^2}{2} + \gamma^2 c - 2c\gamma z}{1-2c}\right)(\mathrm{RV}^c_t + \mathrm{RV}^j_t)} | \mathcal{F}_{t-1}\right] \\
&= \mathbb{E}^{\mathbb{P}}\left[\mathrm{e}^{zr - \frac{1}{2}\ln(1-2c) + \left(z\lambda_c + b_1 + \frac{\frac{z^2}{2} + \gamma^2 c - 2c\gamma z}{1-2c}\right)\mathrm{RV}^c_t + \left(z\lambda_j + b_2 + \frac{\frac{z^2}{2} + \gamma^2 c - 2c\gamma z}{1-2c}\right)\mathrm{RV}^j_t} | \mathcal{F}_{t-1}\right] \\
&= \mathrm{e}^{zr - \frac{1}{2}\ln(1-2c)} \mathbb{E}^{\mathbb{P}}\left[\mathrm{e}^{\left(z\lambda_c + b_1 + \frac{\frac{z^2}{2} + \gamma^2 c - 2c\gamma z}{1-2c}\right)\mathrm{RV}^c_t} | \mathcal{F}_{t-1}\right] \mathbb{E}^{\mathbb{P}}\left[\mathrm{e}^{\left(z\lambda_j + b_2 + \frac{\frac{z^2}{2} + \gamma^2 c - 2c\gamma z}{1-2c}\right)\mathrm{RV}^j_t} | \mathcal{F}_{t-1}\right] .
\end{aligned} \tag{10}$$

In the third line we have used the result that if $Z \sim \mathcal{N}(0,1)$ then

$$\mathbb{E}\left[\exp\left(x\left(Z+y\right)^2\right)\right] = \exp\left(-\frac{1}{2}\ln\left(1-2x\right) + \frac{xy^2}{1-2x}\right).$$

For a noncentred gamma random variable, from [33] we know that

$$\mathbb{E}^{\mathbb{P}}\left[e^{x_1 \mathrm{RV}^c_t} | \mathcal{F}_{t-1}\right] = \exp\left(-\delta\mathcal{W}\left(x_1,\theta\right) + \mathcal{V}\left(x_1,\theta\right)\left(d + \sum_{i=1}^{p} \beta_i \mathrm{RV}^c_{s-i} + \sum_{j=1}^{q} \alpha_j \ell_{s-j}\right)\right) ,$$

where

$$\mathcal{V}(x_1,\theta) = \frac{\theta x_1}{1-\theta x_1}, \quad \mathcal{W}(x_1,\theta) = \ln(1 - x_1\theta),$$

and

$$x_1(z,b_1,c) = z\lambda_c + b_1 + \frac{\frac{1}{2}z^2 + \gamma^2 c - 2c\gamma z}{1-2c}\,. \tag{11}$$

For the computation of the last expectation in the final line of (10), we use the property that if Z_t is a compound Poisson process with rate ω and *i.i.d.* jump sizes D_i, then

$$\mathbb{E}\left[e^{xZ_t}|\mathcal{F}_{t-1}\right] = \exp\left(\omega\left(M_D(x)-1\right)\right), \tag{12}$$

where $M_D(x)$ is the MGF of the jump size random variable D. Since sizes are distributed according to a gamma distribution, we have

$$M_D(x) = \frac{1}{\left(1-x\tilde{\theta}\right)^{\tilde{\delta}}}\,. \tag{13}$$

From expressions (12) and (13) we obtain

$$\mathbb{E}^{\mathbb{P}}\left[e^{x_2 \mathrm{RV}^j_t}|\mathcal{F}_{t-1}\right] = \exp\left(\tilde{\Theta}\mathcal{J}\left(x_2,\tilde{\theta},\tilde{\delta}\right)\right),$$

where

$$\mathcal{J}(x_2,\tilde{\theta},\tilde{\delta}) = \frac{1-(1-\tilde{\theta}x_2)^{\tilde{\delta}}}{(1-\tilde{\theta}x)^{\tilde{\delta}}} \quad \text{and} \quad x_2(z,b_2,c) = z\lambda_j + b_2 + \frac{\frac{1}{2}z^2 + \gamma^2 c - 2c\gamma z}{1-2c}\,.$$

Gathering all the previous results, we finally conclude

$$\begin{aligned}
&\mathbb{E}^{\mathbb{P}}\left[e^{zy_t + \mathbf{b}\cdot\mathbf{RV}_t + c\ell_t}|\mathcal{F}_{t-1}\right] = \\
&\exp\Bigg[zr - \frac{1}{2}\ln(1-2c) + \mathcal{V}(x_1,\theta)\left(d + \sum_{i=1}^{p}\beta_i \mathrm{RV}^c_{t-i} + \sum_{j=1}^{q}\alpha_j\ell_{t-j}\right) \\
&-\delta\mathcal{W}(x_1,\theta) + \tilde{\Theta}\mathcal{J}(x_2,\tilde{\theta},\tilde{\delta})\Bigg]\,.
\end{aligned}$$

The direct comparison of the last expression with (9) allows to derive the following explicit expressions

$$\mathcal{A}(z,\mathbf{b},c) = zr - \frac{1}{2}\ln(1-2c) - \delta\mathcal{W}(x_1,\theta) + d\mathcal{V}(x_1,\theta) + \tilde{\Theta}\mathcal{J}(x_2,\tilde{\theta},\tilde{\delta})\,, \tag{14}$$

$$\mathcal{B}_i(z,b_1,c) = \mathcal{V}(x_1,\theta)\beta_i\,, \tag{15}$$

$$\mathcal{C}_j(z,b_1,c) = \mathcal{V}(x_1,\theta)\alpha_j\,. \tag{16}$$

As shown in [41], once we have above expressions we obtain

$$\phi^{\mathbb{P}}(t,T,z) = \mathbb{E}^{\mathbb{P}}\left[e^{zy_{t,T}}|\mathcal{F}_t\right] = \exp\left(\mathrm{a}_t + \sum_{i=1}^{p}\mathrm{b}_{t,i}\mathrm{RV}^c_{t+1-i} + \sum_{i=1}^{q}\mathrm{c}_{t,i}\ell_{t+1-i}\right)$$

where

$$\begin{aligned}
\mathrm{a}_s &= \mathrm{a}_{s+1} + zr - \frac{1}{2}\log(1-2\mathrm{c}_{s+1,1}) + d\mathcal{V}(\mathrm{x}^c_{s+1},\theta) - \delta\mathcal{W}(\mathrm{x}^c_{s+1},\theta) + \tilde{\Theta}\mathcal{J}(\mathrm{x}^j_{s+1},\tilde{\theta}) \\
\mathrm{b}_{s,i} &= \begin{cases}\mathrm{b}_{s+1,i} + \mathcal{V}(\mathrm{x}^c_{s+1},\theta)\beta_i & for\ 1 \le i \le p-1 \\ \mathcal{V}(\mathrm{x}^c_{s+1},\theta)\beta_i & for\ i = p\end{cases} \\
\mathrm{c}_{s,i} &= \begin{cases}\mathrm{c}_{s+1,i} + \mathcal{V}(\mathrm{x}^c_{s+1},\theta)\alpha_i & for\ 1 \le i \le q-1 \\ \mathcal{V}(\mathrm{x}^c_{s+1},\theta)\alpha_i & for\ i = q\end{cases}
\end{aligned} \tag{17}$$

with

$$\mathrm{x}^c_{s+1} = z\lambda_c + \mathrm{b}_{s+1,1} + \frac{\frac{1}{2}z^2 + \gamma^2 \mathrm{c}_{s+1,1} - 2\mathrm{c}_{s+1,1}\gamma z}{1 - 2\mathrm{c}_{s+1,1}}\,, \tag{18}$$

$$\mathrm{x}^j_{s+1} = z\lambda_j + \frac{\frac{1}{2}z^2 + \gamma^2 \mathrm{c}_{s+1,1} - 2\mathrm{c}_{s+1,1}\gamma z}{1 - 2\mathrm{c}_{s+1,1}}\,. \tag{19}$$

The functions $\mathcal{V}$, $\mathcal{W}$ and $\mathcal{J}$ are defined as above. The terminal conditions read $\mathrm{a}_T = \mathrm{b}_{T,i} = \mathrm{c}_{T,j} = 0$ for $i = 1, 2, ..., p$ and $j = 1, 2, ..., q$.

B No-arbitrage condition

The no-arbitrage conditions are

$$\begin{aligned} \mathbb{E}^{\mathbb{P}}\left[M_{s,s+1} | \mathcal{F}_s\right] &= 1 \text{ for } s \in \mathbb{N}\,, \\ \mathbb{E}^{\mathbb{P}}\left[M_{s,s+1} e^{y_{s+1}} | \mathcal{F}_s\right] &= \mathrm{e}^r \text{ for } s \in \mathbb{N}. \end{aligned} \tag{20}$$

The first relation is satisfied by definition of $M_{s,s+1}$. From a general result in [41], condition (20) is satified if, and only if

$$\begin{aligned} \mathcal{A}(1-\nu_y, -\boldsymbol{\nu}, 0) &= r + \mathcal{A}(-\nu_y, -\boldsymbol{\nu}, 0)\,, \\ \mathcal{B}_i(1-\nu_y, -\boldsymbol{\nu}, 0) &= \mathcal{B}_i(-\nu_y, -\boldsymbol{\nu}, 0)\,, \\ \mathcal{C}_j(1-\nu_y, -\boldsymbol{\nu}, 0) &= \mathcal{C}_j(-\nu_y, -\boldsymbol{\nu}, 0)\,, \end{aligned}$$

with $\boldsymbol{\nu} = (\nu_c, \nu_j)$. To conclude, it is sufficient to show under which conditions the following two relations hold true

$$\begin{aligned} x_1(1-\nu_y, -\nu_c, 0) &= x_1(-\nu_y, -\nu_c, 0)\,, \\ x_2(1-\nu_y, -\nu_j, 0) &= x_2(-\nu_y, -\nu_j, 0)\,. \end{aligned}$$

Simple computations show that the latter equations are satisfied if and only if

$$\nu_y = \lambda_c + \frac{1}{2} = \lambda_j + \frac{1}{2}.$$

Remarkably, the only specification for the log-return dynamics in Eq. (2) which ensures consistency with no-arbitrage is the dynamics where the equity premia λ_c and λ_j are equal and coincide to λ. Then, we obtain

$$\nu_y = \lambda + \frac{1}{2}\,.$$

It is important to notice that the no-arbitrage condition for the equity premium does not constrain the value of the variance risk premia ν_c and ν_j.

C Risk-neutral dynamics

JLHARG models imply a risk-neutral MGF for log-returns whose exponential affine terms can be re-parametrized in order to obtain an expression formally equivalent to the physical MGF. Firstly we observe that the risk-neutral MGF can be expressed with a recursive set of expressions, involving a combination of the functions $\mathcal{A}$, $\mathcal{B}_i$, $\mathcal{C}_j$. Then, recalling the results given in [41], the MGF for JLHARG model under measure $\mathbb{Q}$ has the following form

$$\phi^{\mathbb{Q}}_{\nu_c\,\nu_j\,\nu_y}(t,T,z) = \mathbb{E}^{\mathbb{Q}}\left[e^{z y_{t,T}} | \mathcal{F}_t\right] = \exp\left(\mathrm{a}^*_t + \sum_{i=1}^{p} \mathrm{b}^*_{t,i} \mathrm{RV}^c_{t+1-i} + \sum_{i=1}^{q} \mathrm{c}^*_{t,i} \ell_{t+1-i}\right)\,,$$

where

$$\begin{aligned}
\mathrm{a}_s^* &= \mathrm{a}_{s+1}^* + zr - \frac{1}{2}\log(1-2\mathrm{c}_{s+1,1}^*) + d\mathcal{V}(\mathrm{x}_{s+1}^{c\,*},\theta) - d\mathcal{V}(\mathrm{y}_{s+1}^{c\,*},\theta) \\
&- \delta\mathcal{W}(\mathrm{x}_{s+1}^{c\,*},\theta) + \delta\mathcal{W}(\mathrm{y}_{s+1}^{c\,*},\theta) + \tilde{\Theta}\mathcal{J}(\mathrm{x}_{s+1}^{j\,*},\tilde{\theta}) - \tilde{\Theta}\mathcal{J}(\mathrm{y}_{s+1}^{j\,*},\tilde{\theta}) \\
\mathrm{b}_{s,i}^* &= \begin{cases} \mathrm{b}_{s+1,i}^* + \left(\mathcal{V}(\mathrm{x}_{s+1}^{c\,*},\theta) - \mathcal{V}(\mathrm{y}_{s+1}^{c\,*},\theta)\right)\beta_i & for\ 1 \le i \le p-1 \\ \left(\mathcal{V}(\mathrm{x}_{s+1}^{c\,*},\theta) - \mathcal{V}(\mathrm{y}_{s+1}^{c\,*},\theta)\right)\beta_i & for\ i = p \end{cases} \\
\mathrm{c}_{s,j}^* &= \begin{cases} \mathrm{c}_{s+1,j}^* + \left(\mathcal{V}(\mathrm{x}_{s+1}^{c\,*},\theta) - \mathcal{V}(\mathrm{y}_{s+1}^{c\,*},\theta)\right)\alpha_j & for\ 1 \le j \le q-1 \\ \left(\mathcal{V}(\mathrm{x}_{s+1}^{c\,*},\theta) - \mathcal{V}(\mathrm{y}_{s+1}^{c\,*},\theta)\right)\alpha_j & for\ j = q \end{cases}
\end{aligned} \tag{21}$$

where

$$\begin{aligned}
x_{s+1}^{c\,*} &= (z-\nu_y)\lambda + \mathrm{b}_{s+1,1}^* - \nu_c + \frac{\frac{1}{2}(z-\nu_y)^2 + \gamma^2\mathrm{c}_{s+1,1}^* - 2\mathrm{c}_{s+1,1}^*\gamma(z-\nu_y)}{1-2c_{s+1,1}^*} \\
x_{s+1}^{j\,*} &= (z-\nu_y)\lambda - \nu_j + \frac{\frac{1}{2}(z-\nu_y)^2 + \gamma^2\mathrm{c}_{s+1,1}^* - 2\mathrm{c}_{s+1,1}^*\gamma(z-\nu_y)}{1-2\mathrm{c}_{s+1,1}^*} \\
y_{s+1}^{l\,*} &= -\nu_y\lambda - \nu_l + \frac{1}{2}\nu_y^2,
\end{aligned}$$

with $l = c, j$ and the terminal conditions are $\mathrm{a}_T^* = \mathrm{b}_{T,i}^* = \mathrm{c}_{T,j}^* = 0$ for $i = 1, 2, ..., p$ and $j = 1, 2, ..., q$.

The first passage consists in comparing expression (21) with (17). We have to find a set of new parameters for which the recursive expressions for $\mathrm{a}_t^*, \mathrm{b}_t^*, \mathrm{c}_t^*$ under $\mathbb{Q}$ correspond to the expressions under $\mathbb{P}$. We start defining

$$\begin{aligned}
x_{s+1,i}^{c\,**} &= z\lambda^* + b_{s+1,1}^* + \frac{\frac{1}{2}z^2 + (\gamma^*)^2 c_{s+1,1}^* - 2c_{s+1,1}^*\gamma^* z}{1-2c_{s+1,1}^*}, \\
x_{s+1,i}^{j\,**} &= z\lambda^* + \frac{\frac{1}{2}z^2 + (\gamma^*)^2 c_{s+1,1}^* - 2c_{s+1,1}^*\gamma^* z}{1-2c_{s+1,1}^*}.
\end{aligned}$$

Then, the following relations have to hold

$$\delta\left(\mathcal{W}\left(\mathrm{x}_{s+1}^{c\,*},\theta\right) - \mathcal{W}\left(\mathrm{y}^{c\,*},\theta\right)\right) = \delta^*\mathcal{W}\left(\mathrm{x}_{s+1}^{c\,**},\theta^*\right) \tag{22}$$

$$\beta_i\left(\mathcal{V}\left(\mathrm{x}_{s+1}^{c\,*},\theta\right) - \mathcal{V}\left(\mathrm{y}^{c\,*},\theta\right)\right) = \beta_i^*\mathcal{V}\left(\mathrm{x}_{s+1}^{c\,**},\theta^*\right) \tag{23}$$

$$\alpha_j\left(\mathcal{V}\left(\mathrm{x}_{s+1}^{c\,*},\theta\right) - \mathcal{V}\left(\mathrm{y}^{c\,*},\theta\right)\right) = \alpha_j^*\mathcal{V}\left(\mathrm{x}_{s+1}^{c\,**},\theta^*\right) \tag{24}$$

$$\tilde{\Theta}\left(\mathcal{J}\left(\mathrm{x}_{s+1}^{j\,*},\tilde{\theta}\right) - \mathcal{J}\left(\mathrm{y}^{j\,*},\tilde{\theta}\right)\right) = \tilde{\Theta}^*\mathcal{J}\left(\mathrm{x}_{s+1}^{j\,**},\tilde{\theta}^*\right) \tag{25}$$

with $\mathrm{y}^{c\,*} = -\lambda^2/2 - \nu_c + \frac{1}{8}$ and $\mathrm{y}^{j\,*} = -\lambda^2/2 - \nu_j + \frac{1}{8}$.
Equation (22) can be explicitly written as

$$\delta\log\left[1 - \frac{\theta}{1-\theta\mathrm{y}^{c\,*}}\left(\mathrm{x}_{s+1}^{c\,*} - \mathrm{y}^{c\,*}\right)\right] = \delta^*\log\left(1 - \theta^*\mathrm{x}_{s+1}^{c\,**}\right),$$

which implies the following three sufficient conditions

$$\begin{aligned}
\delta^* &= \delta \\
\theta^* &= \frac{\theta}{1-\theta\mathrm{y}^{c\,*}} \\
\mathrm{x}_{s+1}^{c\,**} &= \mathrm{x}_{s+1}^{c\,*} - \mathrm{y}^{c\,*}.
\end{aligned} \tag{26}$$

It can be easily verified that the last condition (26) is satisfied by substituting

$$\lambda_c^* = -\frac{1}{2}\,,$$
$$\gamma^* = \gamma + \lambda + \frac{1}{2}.$$

The equation (23) can be equivalently expressed in the form

$$\frac{\beta_i}{1-\theta \mathrm{y}^{c\,*}}\,\frac{\theta}{1-\theta \mathrm{y}^{c\,*}}\,\frac{\mathrm{x}_{s+1}^{c\,*}-\mathrm{y}^{c\,*}}{1-\theta/(1-\theta \mathrm{y}^{c\,*})\left(\mathrm{x}_{s+1}^{c\,*}-\mathrm{y}^{c\,*}\right)} = \beta_i^*\,\frac{\theta^*\mathrm{x}_{s+1}^{c\,**}}{1-\theta^*\mathrm{x}_{s+1}^{c\,**}}$$

which gives another sufficient condition for the mapping

$$\beta_i^* = \frac{\beta_i}{1-\theta \mathrm{y}^{c\,*}}\,.$$

An analogous consideration about the third condition (24) allows to obtain the condition on α_i^*,

$$\alpha_i^* = \frac{\alpha_i}{1-\theta \mathrm{y}^{c\,*}}\,.$$

Relation (8) gives us the expressions for β_d^*, β_w^*, β_m^*, α_d^*, α_w^* and α_m^*. Finally, equation (25) provides the last sufficient condition

$$\frac{\tilde{\Theta}}{\left(1-\tilde{\theta}\mathrm{y}^{j\,*}\right)^{\tilde{\delta}}}\,\frac{1-\left(\left(1-\tilde{\theta}\mathrm{x}_{s+1}^{j\,*}\right)/\left(1-\tilde{\theta}\mathrm{y}^{j\,*}\right)\right)^{\tilde{\delta}}}{\left(\left(1-\tilde{\theta}\mathrm{x}_{s+1}^{j\,*}\right)/\left(1-\tilde{\theta}\mathrm{y}^{j\,*}\right)\right)^{\tilde{\delta}}} = \tilde{\Theta}^*\,\frac{1-(1-\tilde{\theta}^*\mathrm{x}_{s+1}^{j\,**})^{\tilde{\delta}^*}}{(1-\tilde{\theta}^*\mathrm{x}_{s+1}^{j\,**})^{\tilde{\delta}^*}}\,,$$

which is satisfied if

$$\begin{aligned}
\tilde{\delta}^* &= \tilde{\delta}\,,\\
\tilde{\Theta}^* &= \frac{\tilde{\Theta}}{\left(1-\tilde{\theta}\mathrm{y}^{j\,*}\right)^{\tilde{\delta}}}\,,\\
\tilde{\theta}^* &= \frac{\tilde{\theta}}{1-\tilde{\theta}\mathrm{y}^{j\,*}}\,,\\
\mathrm{x}_{s+1}^{j\,**} &= \mathrm{x}_{s+1}^{j\,*}-\mathrm{y}^{j\,*}\,.
\end{aligned} \tag{27}$$

As it can be seen the last condition (27) is redundant when compared to the condition (26).